MRS Advances
https://doi.org/10.1557/s43580-023-00735-7

ORIGINAL PAPER

Addition of activated carbon fiber in the negative plate of lead-acid battery: Effect on the electrochemical and electrical performance

Mariana Silva Morán[1] · Natanael Batista David[2] · Rubens Nunes de Faria Junior[3] · Jossano Saldanha Marcuzzo[4] · Andrés Cuña[5]

Received: 15 June 2023 / Accepted: 28 November 2023

Abstract

In recent years, several scientific works have reported that the addition of carbon materials to the negative electrode in lead-acid batteries can improve the electrical performance of these energy accumulators. In this work, the effect of textile polyacrylonitrile derived activated carbon fiber (ACF), used before as reusable adsorbents of pharmaceutical compounds, to the negative plate of a lead-acid battery was studied. The physicochemical and electrochemical properties of a negative plate with addition of 0.1 (wt%) of ACF and the same plate without addition of ACF were compared. Electrical tests of the ACF containing batteries showed an increase in the number of charge/discharge cycles, between 15.4 and 47.8% higher, compared to the non ACF battery. This improvement would be related to an improvement of the electrochemical (higher charge capacity and lower resistance) and textural (higher specific surface area) properties caused by the addition of the ACF.

Introduction

The development of new technologies related to the generation and storage of energy, and the improvement of existing ones, is a challenge for the current scientific community. Lead-acid batteries are energy storage devices widely used in vehicular mobility and other applications that require the accumulation/supply of electrical energy [1]. Basically, they are composed of a Pb electrode (negative plate) and a PbO_2 electrode (positive plate) immersed in a sulfuric acid solution [2]. Although battery technology and commercialization are consolidated, new demands related to modern vehicles require improvements in some characteristics of their performance [3]. In the particular case of applications in hybrid electric vehicles, the requirements of these vehicles (more complex from the point of view of electrical demand and with higher energy efficiency requirements), require improvements in the following battery characteristics [1, 2]: (i) useful life; (ii) dynamic load acceptance; (iii) minimize gas formation and water loss (especially when carbon materials are used in the negative plate); (iv) improve performance at elevated temperatures; (v) corrosion suppression during high rate load to partial state of charge cycles (HRPSoC). Under these conditions, lead-acid batteries tend to fail due to sulfation of the negative plate, also causing a disintegration effect between the active material of the electrode and the support. In recent years, different scientific works have reported that the addition of carbon materials to the battery's negative plate can have different beneficial effects on the performance of the final battery [3–7]. It was observed that the increase in the carbon content in the formulation of the negative plates of the batteries increases the battery life cycle by reducing their sulfation [8–11].

On the other hand, the wide diversity of carbonaceous materials, with different physicochemical and electrochemical characteristics, determines a wide universe of possible types of carbon materials that can be used as additive to enhance the performance of negative plate in Lead-acid batteries. The particular characteristics of the carbon material can determine different effects on the physicochemical and electrochemical properties of the negative plate, and the

✉ Mariana Silva Morán
msilva@fing.edu.uy

1 Departamento de Metales, Instituto de Ensayo de Materiales, Universidad de la República – Facultad de Ingeniería, Montevideo, Uruguay

2 Baterias Automotivas Ltda, Apucarana, PR, Brazil

3 Instituto de Pesquisas Energéticas e Nucleares (IPEN), Sao Paulo, Brazil

4 JMHP Consultoria em Materiais Ltd., Jacareí, Brazil

5 Universidad de la República-Facultad de Química, DETEMA, Área Fisicoquímica, Montevideo, Uruguay

Published online: 05 February 2024

electrical performance of the full battery [12]. In this sense, activated carbon fibers may have interesting characteristics for this type of application, such as high specific surface area, adequate pore size distribution and good electrical conductivity [13]. These are desirable for different electrochemical applications related to the electrical energy storage. Rodrigues et al [14] have reported the use of activated carbon fibers obtained from Brazilian textile polyacrylonitrile (PAN), with good electrical and electrochemical properties for supercapacitor electrode applications. However, as far as the authors know, no complete studies have been reported on the use of this type of carbon fiber as additive to improve the performance of negative plates of Lead-acid batteries. In this work, we study the effect of adding a textile PAN derived activated carbon fiber in the negative plate of a Lead-acid battery. Samples of negative plates with and without carbon fiber were compared from the point of view of their physicochemical and electrochemical properties. The influence of in the electrical properties of the full battery was also studied in collaboration with the Brazilian battery company FUSION.

Experimental

Materials preparation

Activated carbon fiber

The lab-made activated carbon felt, herein named Activated Carbon Fiber (ACF), was prepared from 5.0 dtex PAN heavy tow textile fibers following the procedure described for Marcuzzo et al. [13]. To obtain ACF, textile fibers were thermally oxidized in air in an oven between 200 and 300 C. The oxidized PAN textile fiber was made into felt by a standard textile process. Then it was carbonized under a flow of argon at 900C for 20 min, and later it was activated under a flow of CO_2 gas, keeping it at 1000C for 50 min. At the end, the sample is left to cool to room temperature under argon atmosphere.

Lead-acid battery plates

The negative lead-acid battery plates (with and without addition of ACF) were prepared by the Brazilian company FUZION (Baterias Automotivas Ltda, Apucarana—PR), following the usual commercial manufacturing procedure used for the company, using materials, and following procedures and criteria commonly used and accepted worldwide [15]. Briefly, the manufacturing procedure consists of mixing the proper proportions of lead oxide, sulfuric acid, expanders, water and an acrylic fiber. The formed paste is then supported on a lead grid screen. Finally, the obtained paste is subjected to a curing process to obtain the plaque. In the case of the negative plate containing the ACF to be studied, the procedure was as described above, but adding 0.1% by weight of the carbon material in the formulation. Thus, negative plaques were obtained without addition of fiber (Pb) and with addition of fiber (Pb + ACF).

In order to evaluate the electrical performance of the entire battery using prepared negative plates, positive plates were also prepared following the usual materials and procedure used for the company.

Physicochemical characterization of the FC and negative plates

The morphology, microstructure and surface chemistry of the samples were analyzed by scanning electron microscopy (SEM). In case of FC, surface was analyzed using an equipment N NovaNanoSEM400 with an acceleration voltage of 20 kV, and the negatives plates were analyzed using a Jeol 5900 equipped with an energy dispersive X-ray spectroscopy (EDS) analysis probe. The textural characteristics of the samples were evaluated by adsorption–desorption isotherms of N_2 at 77 K, using a Micromeritics ASAP2010 adsorption equipment for the FC and a Micromeritics ASAP2020 adsorption equipment for the negative plate. Before the experiments, degasification of the samples was performed at 200 °C and vacuum for 12 h. The BET specific surface area (S_{BET}) of the samples was determined by the Brunauer–Emmett–Teller (BET) method. The total pore volume (V_T) was calculated from the amount of N_2 adsorbed at relative pressure around 0.99, and the average pore size was calculated according to the Eq. 1:

$$d_p(\text{nm}) = \frac{4000 V_T}{S_{BET}} \quad (1)$$

where dp is the average pore size, V_T ($cm^3\ g^{-1}$) is the total pore volume and S_{BET} ($m^2\ g^{-1}$) is the specific surface area of the sample.

Electrochemical characterizations of the negative plates in three-electrode cell configuration

The electrochemical performance of the prepared negative plates, was evaluated using a conventional three electrodes cell. A certain amount of the prepared plate (active material + grid) was used as a working electrode. Platinum wire and Hg/Hg_2SO_4 (Sat.) were used as counter and reference electrode, respectively. A 5 mol L^{-1} solution of aqueous sulfuric acid solution was used as electrolyte. The samples were analyzed by cyclic voltammetry (VC) experiment in the range of − 0.5 to − 1.25 V *vs.* Hg/Hg_2SO_4 at scan rate of 10 mV s^{-1}. Electrochemical impedance spectroscopy (EIS)

characterizations were performed at − 0.9 V *vs.* Hg/Hg_2SO_4, applying a potential wave with an amplitude of 10 mV, in the frequency range from 100 kHz to 0.01 Hz. All measurements were performed at room temperature and using a potentiostat/galvanostat/ZRA (Interface 1010E from Gamry Instruments).

Lead-acid battery electrical tests in full cell configuration

The electrical performance of the lead-acid batteries in the full cell configuration was evaluated under the EN 50342-6/2015 standard. Batteries were assembled according to the usual procedure using the positive and negative plates. One group of batteries were assembled with the Pb sample as negative plates, and another with the ACF sample.

The life cycle test was carried out at 17.5% depth of discharge (DOD) per the above standard. In this test, from the charged battery, a pre-discharge of $4C_{20}$ is applied for 2.5 h to reach 50% of the state of charge with respect to the nominal capacity of the battery. Then, 85 charge and discharge cycles are carried out, the charge is carried out at $7C_{20}$ for 40 min limiting the voltage to 14.4 V and the discharge is carried out at $7C_{20}$ for 30 min.

Once the 85 cycles are finished, the following steps are carried out:

1. Equalization charge at $2C_{20}$ and constant voltage of 15.6 V for 18 h.
2. Discharge to C_{20} up to 10.5 V.
3. Full recharge at $5C_{20}$ and constant voltage of 15.6 V for 24 h.

Once the test sequence is complete, it is repeated until the batteries reach 10 V when discharged. At this point the test is terminated.

Under these conditions, the batteries are tested working between 50% and 67.5% of their state of charge, with a depth of discharge of 17.5%.

Results and discussion

In Fig. 1a and 1b the SEM micrographs of sample ACC are shown. The typical structure of a carbon cloth is observed. SEM micrographs of the negative plates where obtained before and after the electrochemical charge (by linear sweep voltammtry from − 0.5 to − 1.25 V vs. Hg). Figure 1c and d shows the micrographs obtained for sample Pb before and after charge respectively. The charged Pb sample is formed for irregular porous-spongy like lead structures, while the discharged one present bulkiest particles of $PbSO_4$ formed during the charge reaction. In the micrographs

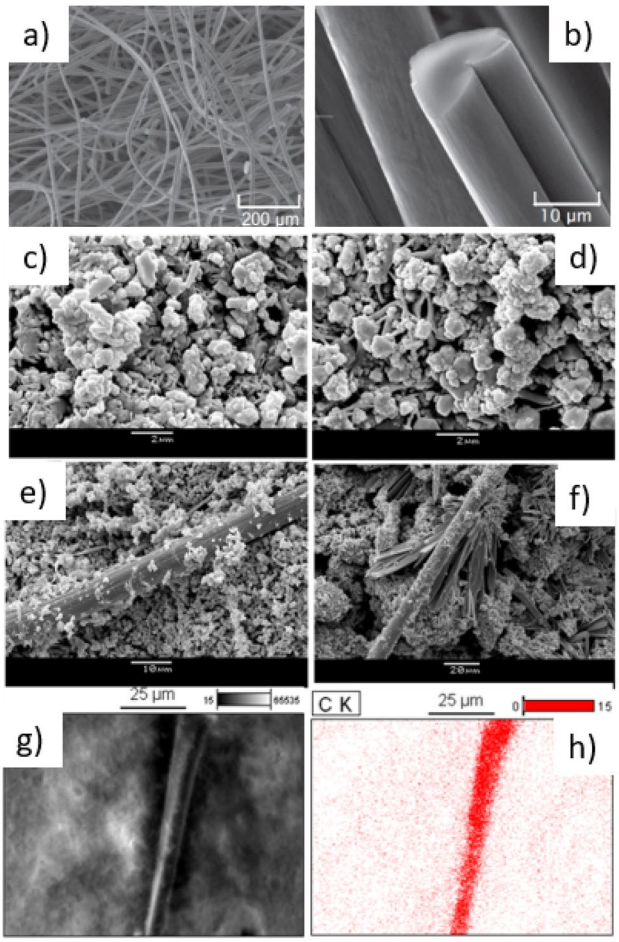

Fig. 1 SEM micrographs of the samples: **a** and **b** ACF **c** Discharged Pb sample; **d** Charged Pb sample; **e** Discharged Pb + ACF sample; **f** Charged Pb + ACF sample; **g** and **h** EDS carbon mapping for the Pb + FCA sample

corresponding to the Pb + ACF sample (see Fig. 1e and f) the presence of a filament is clearly distinguished. This size is clearly larger than that of the acrylic fiber added as structural support during negative plate preparation. The ESD mapping performed on the observed fiber show higher carbon content which confirms that this filament correspond to the studied ACF (see Fig. 1g and h). The Fig. 1e and f can also confirm that the fiber is well dispersed inside the paste, intimately combining with the active material of the plate. In other hand, smaller filaments of the acrylic fiber used in the negative plate preparation can be observed in both samples. On the other hand, it is interesting to note that the charged Pb + ACF sample (see Fig. 1f) presents the formation of long and laminar crystals around to the ACF filaments, likely from $PbO{\cdot}PbSO_4$ [16].

Adsorption–desorption isotherms obtained for the both samples for negative plates presents a type III isotherm, while de ACF presents a type I. The textural parameters

obtained from these isotherms (see Table 1) show S_{BET} values similar to those reported for this type of Pb materials [17]. Compared with Pb sample, Pb + ACF has a slightly larger surface area but with a lower dp. Although the amount of ACF in the Pb + ACF sample is low (0.1%), the high specific surface area of this fiber could determine the highest area value observed. On the other hand, the ACF could favor the decrease of the size of Pb aggregates and block the pores between them [17]. This last combined with the high microporosity of the ACF can determine the decrease in the pore size of the Pb + ACF with respect to the Pb sample.

The voltamograms obtained for the negative plates from the electrochemical characterization in three-electrode cell configuration are shown in Fig. 2a. The voltammograms have the characteristic shape for this type of material, with an anodic peak related to the Pb oxidation to form $PbSO_4$ and cathodic peak corresponding to the inverse reaction [17–20]. Comparing the area under the peak in the anodic scan (discharge) and the maximum peak current, parameters directly related to the material's charge accumulation capacity, it can be observed that the Pb + ACF sample presented higher area and current density in the peak, indicating that this material has higher electrical storage capacity and efficiency [18]. The ratio of anodic peak current to cathodic peak current (I_{pa}/I_{pc}) is 1.32 and 0.76 for the Pb and Pb + ACF sample respectively. The higher value obtained for the Pb sample shows that this negative plate has less reversibility. On the other hand, the lower I_{pa}/I_{pc} observed for the negative plate containing ACF would be related to a certain difficulty for the oxidation of the Pb formed during charge step. On the other hand, during the discharge in the voltammogram of the Pb + ACF sample it is possible to observe a small peak in the range of − 0.9 to − 1.0 V *vs.* Hg/Hg_2SO_4, possibly related to the electrochemical reduction of $PbO{\cdot}PbSO_4$. This is consistent with what was observed in the Fig. 1d, where the presence of particles with morphological characteristics similar to $PbO{\cdot}PbSO_4$ could be observed. Therefore, it is possible that for the Pb + ACF sample, portion of the $PbO{\cdot}PbSO_4$ formed in the discharge does not completely reduce in the charge step.

Figure 2b shows the Nyquist diagram obtained for the samples at − 0.9 V. It is clearly seen that the charge transfer resistance (R_{CT}) of the Pb sample is much higher than that observed for the Pb + ACF, again demonstrating

Table 1 Textural parameters of the samples

Sample	$S_{BET}/m^2\ g^{-1}$	$V_T/cm^3\ g^{-1}$	d_p/nm
ACF	1,280	0.597	1.87
Pb	1.5	0.019	49.6
Pb + ACF	1.9	0.017	35.6

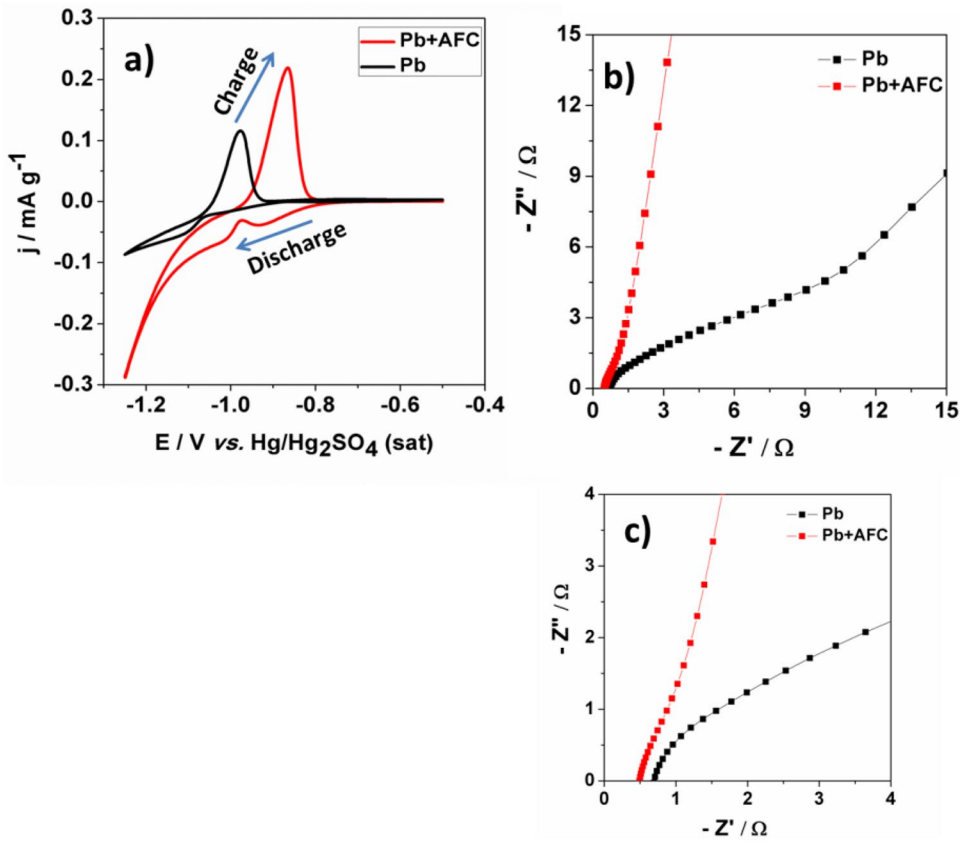

Fig. 2 **a** Voltamograms obtained at 10 mV s^{-1}. **b** Nyquist diagram obtained for the samples at − 0.9 V *vs.* Hg/Hg_2SO_4. **c** High frequency region of the Nyquist diagram obtained for the samples

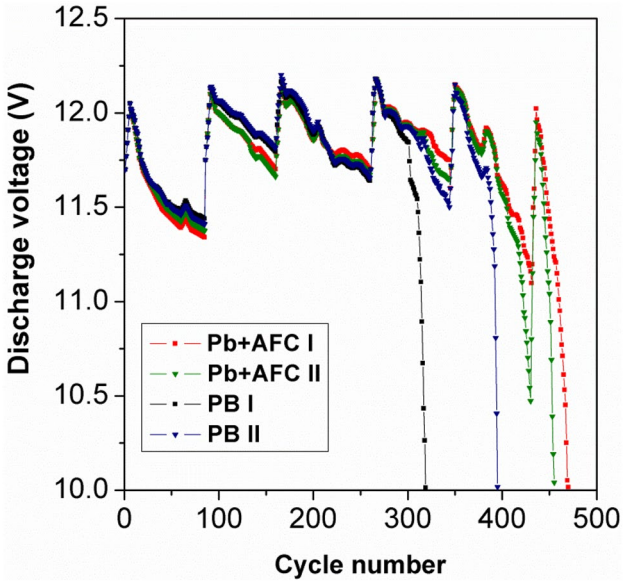

Fig. 3 Discharge voltage vs number of cycle obtained from the electrical test under EN 50342-6/2015 for the samples with and without AFC

that the addition of ACF has had a positive effect on the electrochemical behavior of the negative plate. Figure 2c shows the high frequency area of the Nyquist diagram. The value of intersection with the x-axis can be correlated with the series resistance of the cell, mainly related to the sum of the material and electrolyte resistance (R_S). The negative plate with ACF showed a value of $R_S = 0.5\ \Omega$, lower than the sample plate without ACF ($Rs = 0.7\ \Omega$). Considering that the electrolyte resistance must be the same in both cases, the observed difference can be attributed to differences in the electrical and contact conductivity of the analyzed material, possibly due to the high electrical conductivity presented by the analyzed ACF.

Figure 3 shows the results obtained from the test of the EN 50342-6/2015 standard for lead-acid batteries in the full cell configuration. The results of this test show that batteries assembled with negative plates containing AFCs (Pb + AFC I and Pb + AFC II) reach 470 and 455 cycles before reaching 10 V at discharge potential. Batteries assembled with negative plates without added fiber (Pb I, Pb II) reach 318 and 394 cycles before reaching 10 V at discharge potential. This represents an increase between 15.4% and 47.8% in the number of life cycles of batteries containing negative plates with AFC. The ACF acts as a porous skeleton that facilitates the electrolyte diffusion. Also provides sites for crystallization and dissolution of lead sulfate, preventing the formation of large lead sulfate crystals that are more difficult to dissolve [10].

Conclusions

SEM micrographs and EDS analysis confirm the adequate incorporation of the ACF into the internal structure of the negative plate of the lead-acid battery. These fibers are clearly distinguished from structural acrylic fibers by their larger filament diameter and higher carbon content. In both analyzed samples the a spongy-like lead is the main active material in the charge state while bulkiest $PbSO_4$ compound is present in the discharged plates. For the Pb + ACF sample in the charged state, particles of $PbO{\cdot}PbSO_4$ are observed. For the negative plate with ACF, higher S_{BET} value and a smaller pore size were observed. Cyclic voltammetry performed in the three-electrode configuration shows a higher electrochemical activity related to the charge–discharge redox reaction for the Pb + ACF sample associated with the $Pb/PbSO_4$ pair. A smaller redox peak associated with the reduction of the $PbO{\cdot}PbSO_4$ compound is also observed for this sample. The EIS results indicate that the ACF sample has lower electrochemical resistance linked to the electrical conductivity of the material and the charge transfer resistance. The addition of the ACF on the negative plate improves the electrical performance of the negative plate of the full battery, increasing the number of its life cycle. This would be related to an improvement in the above mentioned textural and electrochemical properties of the material.

Acknowledgments The authors are especially grateful to Prof. Alejandro Amaya—Area Fisicoquímica/DETEMA, Facultad de Química, Universidad de la República, Montevideo, Uruguay for performing the textural analysis. Mariana Silva and Andrés Cuña thank the Uruguayan PEDECIBA-Química for founding.

Author contributions Conceptualization and methodology, MSM, NBD, RNdeFJ, JSM and AC; resources, NBD, JSM and AC; writing MSM, JSM and AC; review and editing, MS and AC.

Funding Not applicable.

Data availability All data generated or analyzed during this study are included in this published article.

Declarations

Conflict of interest The corresponding author declares that there is no conflict of interest.

References

1. J. Garche, E. Karden, P.T. Moseley, D.A.J. Rand, *Lead Acid Batteries for Future Automobiles* (Elsevier, Amsterdam, 2017)
2. R. Faria, L. Zarpelon, M. Serna. Baterias Recarregáveis: Introdução aos materiais e cálculos. Artbiler, Sao Paulo, 2014.
3. P. Moseley, D. Rand, A. Davidson, B. Monahov, Understanding the functions of carbon in the negative active-mass of the

lead–acid battery: A review of progress. J. Energy Storage **19**, 272–290 (2018)
4. P. Tong, R. Zhao, R. Zhang, F. Yi, G. Shi, A. Li, Characterization of lead (II)-containing activated carbon and its excellent performance of extending lead-acid battery cycle life for high-rate partial-state-of-charge operation. J. Power. Sources **286**, 91–102 (2015)
5. L. Flores, G. López, S. García, R. Flores, M. Videa, Construction and characterization of lead acid negative active material+carbon paste electrodes. ECS Trans. **36**(1), 29–35 (2011)
6. X. Zou, Z. Kang, D. Shu, Y. Liao, Y. Gong, C. He, J. Hao, Y. Zhong, Effects of carbon additives on the performance of negative electrode of lead-carbon battery. J. Electrochim. Acta **151**, 89–98 (2015)
7. S. Zhang, H. Zhang, W. Xue, J. Cheng, W. Zhang, G. Cao, H. Zhao, Y. Yang, A layered-carbon/PbSO4 composite as a new additive for negative active material of lead-acid batteries. J. Electrochim. Acta **290**, 46–64 (2018)
8. P. Moseley, Consequences of including carbon in the negative plates of Valve-regulated Lead-Acid batteries exposed to high-rate partial-state-of-charge operation. J. Power. Sources **191**, 134–138 (2009)
9. F. Saeza, B. Martinez, D. Marin, P. Spinelli, F. Trinidad, The influence of different negative expanders on the performance of VRLA single cells. J. Power. Sources **95**(1–2), 174–190 (2001)
10. J. Xiang, P. Ding, H. Zhang, Wu. Xianzhang, J. Chen, Y. Yang, Beneficial effects of activated carbon additives on the performance of negative lead-acid battery electrode for high-rate partial-state-of-charge operation. J. Power. Sources **241**, 150–158 (2013)
11. Z. Lin, N. Lin, H. Lin, W. Zhang, Significance of PbO deposition ratio in activated carbon-based lead carbon composites for lead-carbon battery under high-rate partial state-of-charge operation. J. Electrochim, Acta **338**, 135868 (2020)
12. D. Pavlov, P. Nikolov, G. Petkova, Mechanism of action of electrochemically active carbons on the processes that take place at the negative plates of lead-acid batteries. J. Power. Sources **191**, 58–75 (2009)
13. J. Saldanha, M. Choyu, O. Heitor, A. Polidoro, S. Otani, Influence of thermal treatment on porosity formation on carbon fiber from textile PAN. Mater. Res. **16**, 137–144 (2013)
14. A.C. Rodriguesa, E.L. da Silva, S.F. Quirino, A. Cuña, J.S. Marcuzzo, J.T. Matsushima, E.S. Gonçalvesa, M.R. Baldan, Ag@ activated carbon felt composite as electrode for supercapacitors and a study of three different aqueous electrolytes. Mater. Res. **22**(1), e20180530 (2019)
15. J. Jung, L. Zhang, J. Zhang, *Lead-Acid Battery Technologies. Fundamentals, Materials, and Applications* (Taylor & Francis Group, New York, 2016)
16. S.A.A. Sajadi, A comparative investigation of lead sulfate and lead oxide sulfate study of morphology and thermal decomposition. Am. J. Anal. Chem. **2**, 206–211 (2011)
17. H. Yang, Y. Qiu, X. Guoa, Lead oxide/carbon black composites prepared with a new pyrolysis-pickling method and their effects on the high-rate partial-state-of-charge performance of lead-acid batteries. Electrochim. Acta **235**, 409–421 (2017)
18. H. Wang, Z. Liu, Q. Liang, H. Zhong, G.-C. Han, S. Zhang, Z. Chen, A facile method for preparation of doped-N carbon material based on sisal and application for lead-carbon battery. J. Clean. Prod. **197**, 332–338 (2018)
19. J. Tai, F. Li, Y. Zhou, Z. Fan, H. Wei, D. Zhang, L. Lei, Synthesis and characterisation of tribasic lead sulphate as the negative active material of lead-acid battery. J. Solid State Electrochem. (2018). https://doi.org/10.1007/s10008-018-3998-8
20. L. Dong, S. Gao, H. Peng, C. Chen, J. Wang, W. Yan, J.C.-Y. Jung, J. Zhang, Boosting high-rate-partial-state-of-charge performance of lead-acid batteries by incorporating trace amount of sodium dodecyl sulfate modified multi-walled carbon nanotubes into negative active materials. J. Energy Storage **44**, 103402 (2021)